Available online at www.sciencedirect.com
SCIENCE DIRECT
Catalysis Today 99 (2005) 271–283
CATALYSIS TODAY
www.elsevier.com/locate/cattod

Performance of CO preferential oxidation reactor with noble-metal catalyst coated on ceramic monolith for on-board fuel processing applications

Rajesh K. Ahluwalia[a,*], Qizhi Zhang[a], Donald J. Chmielewski[b], Kevin C. Lauzze[b], Michael A. Inbody[c]

[a]Nuclear Engineering Division, Argonne National Laboratory, 9700 South Cass Avenue, Argonne, IL 60439, USA
[b]Department of Chemical and Environmental Engineering, Illinois Institute of Technology, Chicago, IL 60616, USA
[c]Materials Science and Technology Division, Los Alamos National Laboratory, Los Alamos, NM 87545, USA

Available online 15 December 2004

Abstract

On-board fuel processors are being developed to provide hydrogen-rich gas to the polymer electrolyte fuel cell automotive propulsion systems. Whereas the anode catalyst in the fuel cell has low tolerance for carbon monoxide, 10–100 ppm, reforming of gasoline and other hydrocarbon fuels generally produces 1–2% of CO. Of the many methods of removing CO from the reformer gas, preferential oxidation (PrOx) of CO over noble-metal catalysts is practiced most frequently. In this paper, we present experimental data for CO conversion on a Pt-based catalyst that is active at room temperature and was coated on a ceramic monolith. The data is used to develop an empirical correlation for selectivity for CO oxidation as a function of CO concentration and oxygen stoichiometry at 30,000–80,000/h space velocity. The selectivity correlation is used in a model to analyze the performance of multi-stage, adiabatic PrOx reactors with heat exchange between the stages to cool the reformate to 100 °C. An optimization algorithm is used to determine the operating conditions that can reduce CO concentration to 10 ppm while minimizing parasitic loss of H_2 in the reformate stream. It is found that the 10 ppm constraint limits the maximum inlet CO concentration to 1.05% in a single-stage reactor and to 3.1% in a two-stage reactor. The results clearly show the incremental reduction in parasitic H_2 loss by addition of second and third stages.

Keywords: CO oxidation; PEMFC; Preferential oxidation

1. Introduction

Polymer electrolyte membrane fuel cells (PEMFC) are being considered as a power source for automotive propulsion because of their low operating temperature (~80 °C), high efficiency, zero or low tailpipe emissions of regulated pollutants, and fast start-up and dynamic response times [1]. Direct hydrogen fuel cell systems are also an essential component of the hydrogen economy—a vision of clean, sustainable energy for future generations [2]. There are, however, many impediments to the use of hydrogen as the on-board fuel, the principal ones being low volumetric density of gaseous hydrogen, perceived safety issues in handling and storing hydrogen, and lack of adequate infrastructure for producing and delivering hydrogen. Building a hydrogen infrastructure will also require huge capital investments that may be difficult to sustain until the problems of hydrogen storage and economics are sufficiently resolved. For these reasons, use of on-board fuel processors for reforming gasoline to produce hydrogen on demand is considered an attractive alternative, at least in the transition period. However, gasoline as fuel for fuel cells has its own set of problems. Gasoline is a difficult fuel to reform as it requires high process temperatures, catalysts and process steam [3]. Fuel cell systems based on gasoline fuel processors also lack the simplicity and efficiency of PEMFC systems based on hydrogen as fuel.

* Corresponding author. Tel.: +1 630 252 5979; fax: +1 630 252 5287.
E-mail address: walia@anl.gov (R.K. Ahluwalia).

0920-5861/$ – see front matter © 2004 Elsevier B.V. All rights reserved.
doi:10.1016/j.cattod.2004.10.015

Gasoline may be reformed into a hydrogen rich gas via steam reforming, partial oxidation reforming or autothermal reforming. Regardless of the reforming technique employed, the reformate gas produced contains 0.5–3% of CO even after the water gas shift step. Carbon monoxide is a poison to the PEMFC stack because it is preferentially adsorbed on to the surface of the Pt-Ru anode catalyst, blocking its access to H_2 and degrading the electrochemical performance of cells operating at temperatures below 100 °C [4–5]. The acceptable CO concentration in the reformate stream is below 10–100 ppm. Higher levels of CO can be tolerated for short bursts of time by bleeding air into the anode passages but the overall performance of the stack suffers.

Carbon monoxide concentration can be reduced from 0.5–3% to 10–100 ppm by selective methanation, pressure swing adsorption, membrane separation, or preferential oxidation (PROx). Selective methanation has the advantage of being a simple and passive technique but even at 100% selectivity for CO conversion (defined as the ratio of H_2 consumed in $CO + 3H_2 = CH_4 + H_2O$ reaction to the total H_2 consumed) consumes 3 mole of H_2 for every mole of CO removed. The actual selectivity for CO conversion in a methanation reactor is less than 100% because of the side reaction between CO_2 and H_2 [6]. Pressure swing adsorption is probably more suited for stationary fuel processor applications because of the requirements of multiple reactor vessels and pressurization [7]. Membrane separation of hydrogen from the reformate stream is another option that is being evaluated [8]. It offers the potential advantage of being able to produce pure hydrogen but at the expense of high operating pressures and costly materials. Because of these limitations in the alternative techniques, preferential oxidation of CO over noble metal catalysts is considered as the most practical scheme for automotive applications [9–12].

The subject of this paper is performance of preferential oxidation reactors with noble metal catalysts wash-coated on to ceramic monoliths. One index that we use for characterizing the performance of a PrOx catalyst is selectivity for CO oxidation (S) defined as the ratio of oxygen consumed by the desired CO reaction to the total oxygen consumed. Another related index is the process stoichiometry λ, which is the ratio of oxygen used in relation to the theoretical amount needed for complete conversion of CO.

From the standpoint of process efficiency, it is desirable to select the PrOx catalyst and operating conditions that lead to S and λ being as close to unity as possible. Additional considerations arise when reforming is to be carried out onboard a vehicle. For fast start, the PrOx reactor must be compact and, in particular, the thermal mass of the catalyst and the components in contact with the flow should be minimized. The catalyst should maintain the fuel processor outlet CO concentration within the fuel cell stack tolerances through the startup transient and transition to normal operation. For cold start, it helps if the catalyst has low light-off temperature for CO oxidation. The catalyst should retain selectivity over the range of temperatures representative of cold start and normal operation. It should be capable of oxidizing high concentrations of CO if the upstream water gas shift reactor is not operating at its optimal temperature as at start-up and during up-load transients.

The purpose of this paper is to present recent results on a low temperature, supported PrOx catalyst that has shown light-off for CO oxidation at room temperature. The focus is on taking data from single-stage PrOx experiments under steady-state conditions and applying them to multi-stage reactors. Particular attention is devoted to determining the operating conditions of one, two and three-stage PrOx reactors that minimize parasitic hydrogen loss while reducing the CO concentrations to a level acceptable by the PEMFC anode electrocatalyst.

2. PrOx experiments

The experimental characterization of the PrOx reactor–catalyst combination was conducted in the PrOx test facility at Los Alamos National Laboratory. The test facility simulates the operating conditions of a PrOx reactor in a fuel processing system. Compressed gas supplies of hydrogen, nitrogen, carbon dioxide, and carbon monoxide are metered through mass flow controllers and mixed to generate the simulated reformate of a fuel processor. Steam is added from a steam generator through metering control valves and a flow meter. Inline gas heaters heat the reformate to the outlet temperature expected from a fuel processor. This simulated reformate then flows through the PrOx reactor test sections. A back-pressure regulator downstream of the PrOx reactor sets the operation pressure within the reactor. The PrOx reactor test section, shown in Fig. 1, can be configured with up to three PrOx reactors connected in series. Each reactor has its own air injection supply and a heat exchanger to control the inlet temperature.

For these experiments, the PrOx reactor was configured with a single catalyst test section with inlet and outlet flow conditioning stages to provide a uniform flow to the catalyst. The catalyst used was an Engelhard Selectra®-PROX I catalyst coated by Engelhard Corporation on a Corning 600 cpsi (cells per square inch) cordierite monolith. The monolith dimensions were 7.62 cm diameter by 12.7 cm long. Temperature profiles were measured by 0.020 in. K-type thermocouples inserted into the monolith channels to depths at 2.54 cm intervals and at the inlet and outlet face of the monolith, as shown in the schematic in Fig. 1. Gas samples were extracted from the inlet stream to the monolith and at the outlet of the monolith for measurements of CO concentration using non-dispersive infrared (NDIR) analyzers and of oxygen concentration using a paramagnetic oxygen analyzer. The NDIR analyzer used to measure CO concentration above 1% had a range of 25,000 ppm with ±250 ppm repeatability. The NDIR analyzer used in experiments with CO concentration below 0.2% had a range of 3000 and ±25 ppm repeatability. The data was

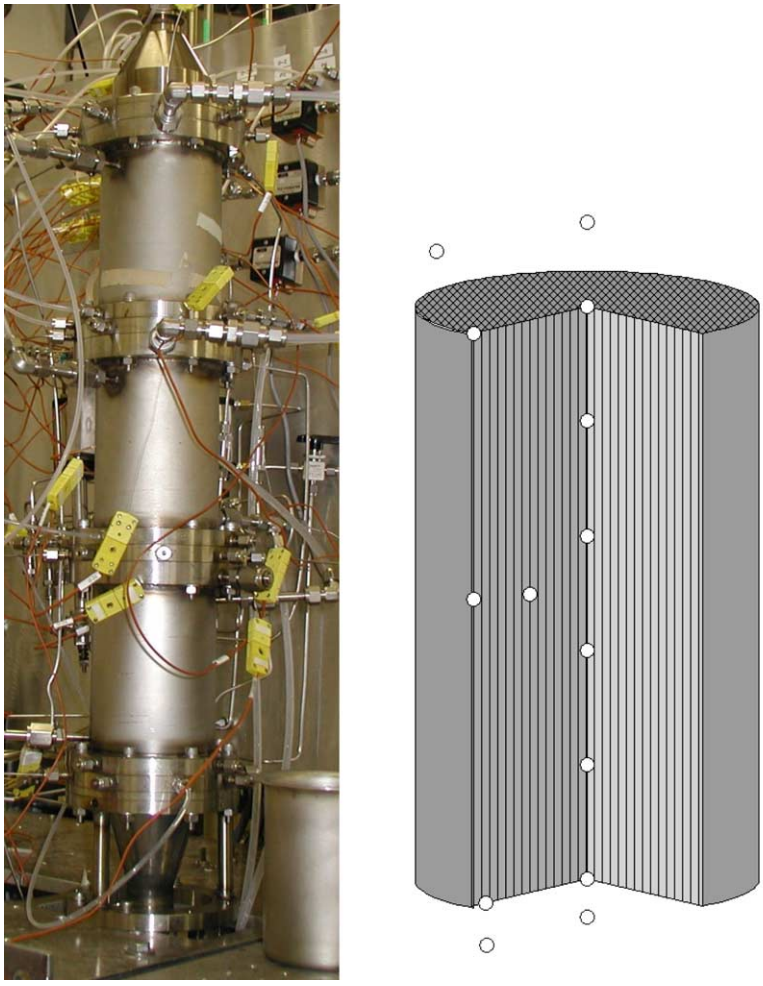

Fig. 1. The experimental PrOx reactor is shown on the left with three stages. The inlet and outlet stages serve as flow conditioning stages. On the right is a schematic cross-section of the catalyst monolith showing the locations of the thermocouples for the temperature profile measurements.

collected under steady-state conditions, i.e., care was taken to ensure all transients had died out before data was recorded.

All tests were conducted at a pressure of 1.5 bar with a dry simulated reformed gas of nominal composition 48% H_2, 30.9% N_2, and balance CO and CO_2. Water concentration was controlled by mixing in steam with the simulated reformed gas upstream of the reactor inlet. The injection of steam caused the inlet gas temperature to vary between 85 and 100 °C. The major gas flows were set and the air injection was varied to obtain measurements over a wide range of oxygen stoichiometry usually to identify the minimum CO concentration. The stoichiometry was limited to keep the outlet temperature below 300 °C.

In all nine series of tests were conducted by varying CO concentration, H_2O concentration, and gas hourly space velocity (GHSV). The test matrix, listed in Table 1, includes three levels of CO concentration (0.2, 1 and 2.6%), two levels of H_2O concentration (0 and 20%), and two levels of space velocity (15,000 and 30,000 h). Addition of steam resulted in the inlet CO concentration varying between 0.17 and 0.2% in the low range and between 1 and 1.3% in the medium range and in the space velocity varying between 31,300 and 38,000/h at high flow rates and between 14,800 and 19,000/h at low flow rates.

Within each series of tests, the oxygen stoichiometry was varied and data was collected for approximately 10 values of λ, between 0.2 and 2.5. In all tests, the outlet oxygen

Table 1
Test Matrix (inlet conditions are concentrations in mole%)

	Case 1	Case 2	Case 3	Case 4	Case 5	Case 6	Case 7	Case 8	Case 9
Inlet CO (%)	2.5	1.3	1.3	1.1	0.2	1.3	0.2	1	0.2
Inlet H_2O (%)	0	0	0	17	17	0	0	20	21
GHSV(1/h)	32000	32000	31000	37000	36000	15000	15000	19000	18000
Oxygen stoichiometry	0.4–1.0	0.4–2.0	0.4–2.0	0.6–2.0	0.2–2.5	0.4–1.3	0.3–2.4	0.6–1.7	0.8–2.2

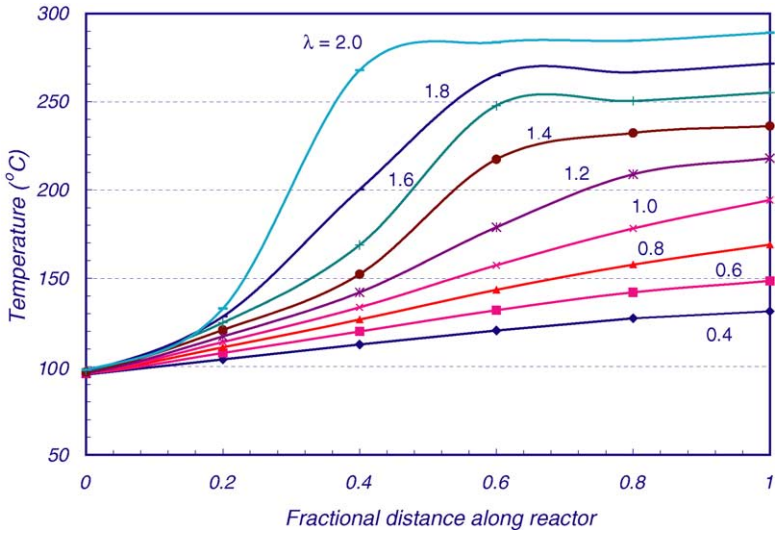

Fig. 2. Measured temperature profiles for experiments in case 2.

concentration was below the detection limit indicating that the added oxygen was completely consumed by the oxidation reactions.

Fig. 2 shows axial temperature profiles from a test series (case 2) with dry reformate, 1.3% inlet CO concentration and 32,000/h space velocity. These are typical of temperature profiles measured for other test cases as well. At the highest stoichiometry, $\lambda = 2$, the temperature profile flattens out mid way through the reactor. The point at which the temperature profile becomes flat moves downstream as λ is reduced. We do not see plateau in temperature profiles for $\lambda < 1$. These results suggest that the oxidation reactions are essentially complete half way across the reactor for $\lambda = 2$, but continue down the length for $\lambda < 1$. They implicitly show the relationship between the minimum space velocity required to complete the PrOx reactions at 1.3% CO and 100 °C inlet temperature. It is emphasized that although the temperature profile increases almost linearly across the reactor for $\lambda = 0.4$, no breakthrough of oxygen was observed. For conditions of case 2 tests, we therefore infer that PrOx reactions on the 600 cpsi monolith support can be completed at a space velocity of 80,000/h at $\lambda = 2$, 53,000/h at $\lambda = 1.8$, 46,000/h at $\lambda = 1.6$, 40,000/h at $\lambda = 1.4$, 36,000/h at $\lambda = 1.2$ and 32,000/h for $\lambda < 1$.

3. PrOx model

Our interest is in developing a correlation for selectivity for CO oxidation as a function of process conditions for the Selectra®-PROX I catalyst coated on a ceramic monolith. We assume that the only competing reactions are

$$CO + \frac{1}{2}O_2 = CO_2$$

$$H_2 + \frac{1}{2}O_2 = H_2O$$

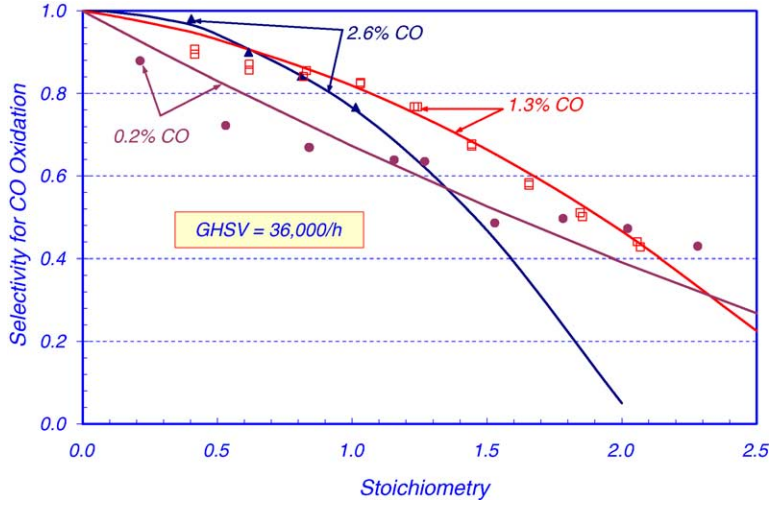

Fig. 3. Measured selectivity for CO oxidation in cases 1, 4, and 5.

so that the selectivity can be determined from the measured change in CO and H_2 molar flow rates across the reactor.

$$S = \frac{\Delta\dot{N}^{CO}}{(\Delta\dot{N}^{CO} + \Delta\dot{N}^{H_2})}$$

Fig. 3 shows the deduced selectivity data for the high flow rate tests, cases 1, 4, and 5, with nominal space velocity between 32,000 and 37,000/h. It is seen that the selectivity for CO oxidation is a strong function of oxygen stoichiometry and inlet CO concentration. For given inlet CO concentration, selectivity always decreases with λ and appears to approach 1 as λ goes to 0. The behavior of selectivity with inlet CO concentration is more complex in that the selectivity curves for different CO concentrations intersect each other. For the conditions of Fig. 3, at fixed λ, selectivity increases with inlet CO concentration for $\lambda < 0.8$. This behavior is consistent with the expectation that the fractional CO coverage of active sites increases with CO concentration making the catalyst more selective to CO oxidation reaction. The situation can reverse at higher λ because of the rise in surface temperature due to the exothermic oxidation reactions (Note that for fixed λ, the extent of exothermic reactions is proportional to the inlet CO concentration.). The higher the surface temperature, the smaller the fractional CO coverage of active sites, and the lower the catalyst selectivity for CO oxidation reaction.

Fig. 4 compares the measured selectivity for two sets of data for 1.3 and 0.2% CO in which the operating conditions are identical except for the moisture content. The data for 1.3% CO are from runs at high flows (cases 3 and 4) and for 0.2% CO from runs at low flows (cases 7 and 9). As mentioned earlier, the variation in space velocity between data at high and low flows are because of addition of steam. The data clearly indicates that for all test conditions moisture has small effect on selectivity for CO oxidation. It implies that at 100–300 °C there is insignificant CO production on the Selectra®-PROX I catalyst by the reverse water gas shift reaction (RWGS).

$$CO_2 + H_2 = CO + H_2O$$

Absence of the RWGS reaction simplifies reactor control and represents a major advantage for a PrOx catalyst that can operate at low temperatures.

Fig. 5 compares the measured selectivity for CO oxidation for two sets of runs in which the operating conditions are identical except for the space velocity. The data for 1.3% CO are from runs at dry condition (cases 3 and 6) and for 0.2% CO from runs with steam (cases 5 and 9). The data indicates that space velocity has a measurable effect on selectivity, particularly at low oxygen stoichiometry. The selectivity is generally higher at 15,000–18,000/h space velocity than at 31,000–36,000/h space velocity. We think that space velocity may influence the selectivity for CO oxidation through mass transfer effects. At high space velocities, CO conversion (and hence overall selectivity) in some portion of the reactor may be limited by mass transfer of CO to the catalyst surface. Because H_2 is in much larger concentration than CO, H_2 conversion is unlikely to be limited by mass transfer through the boundary layer.

For transportation applications we are interested in compact PrOx reactors and therefore in selectivity data at 30,000/h or higher space velocities. Because the selectivity for CO oxidation was seen above to depend weakly on moisture content, we chose to represent S as a function of λ and X, the inlet CO concentration in mole%. We employed a two-step procedure to develop a correlation for $S(\lambda, X)$. In the first step, we correlated S as a function of a reduced parameter λX^n and determined the exponent n so that curves for different inlet CO concentrations do not intersect each other. Fig. 6 shows that a reasonable choice for the exponent n is 0.25. For each inlet CO concentration (2.5, 1.3, and 0.2%), we correlated S as a second-order polynomial in the

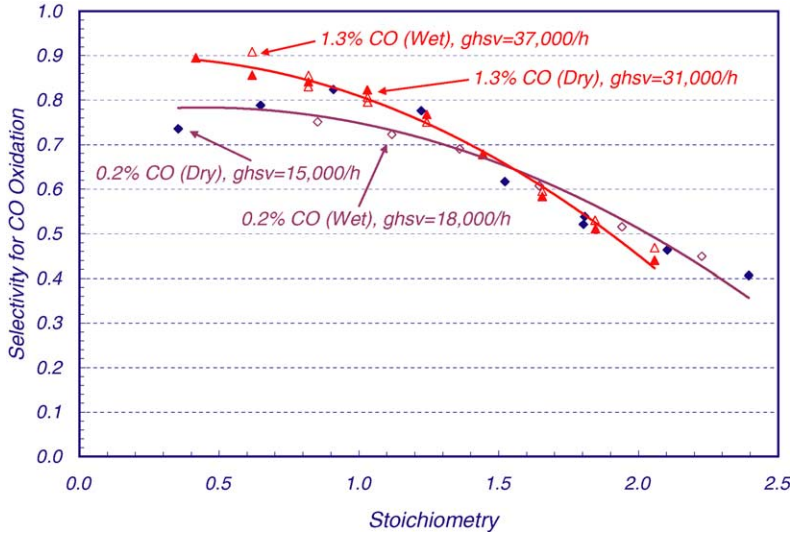

Fig. 4. Effect of steam content on measured selectivity for CO oxidation (cases 3, 4, 7, and 9).

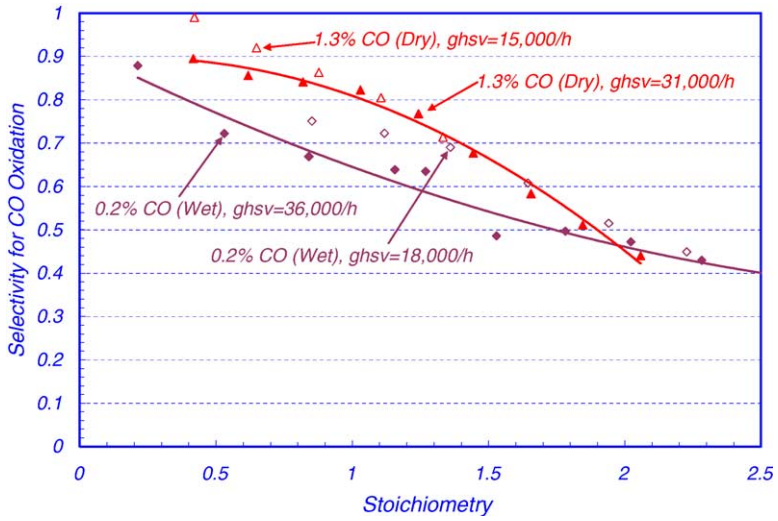

Fig. 5. Effect of GHSV on measured selectivity for CO oxidation (cases 3, 5, 6, and 9).

reduced parameter $\lambda X^{1/4}$, subject to the imposed boundary condition that S approach 1 as λ goes to 0.

$$S = 1 + a(\lambda X^{1/4}) + b(\lambda X^{1/4})^2 \quad (1)$$

The coefficients a and b determined in this manner were different for the three levels of inlet CO concentration. In the second step, we correlated the coefficients a and b themselves by a second-order polynomials in X. A least squares fit analysis gave the following correlations for a and b.

$$a = -0.804 + 0.8034X - 0.1889X^2$$
$$b = 0.2503 - 0.3621X + 0.0802X^2 \quad (2)$$

Together Eqs. (1) and (2) represent a single correlation for selectivity for CO oxidation for SelectraQWQW®-PROX I catalyst coated on the ceramic monolith at 100 °C inlet temperature, 30,000/h nominal space velocity and 0.2–2.5% inlet CO concentration. The goodness of this correlation is tested in Fig. 7 by comparing the exit CO concentration calculated from the correlation with the experimental data.

The comparison in Fig. 7 indicates that our correlation captures all important aspects of the experimental data. Particularly important is the validation of the experimental result for 1.3% inlet CO concentration, which indicates that starting at $\lambda = 0.5$, the exit CO concentration initially decreases with λ, reaches a minimum at $\lambda = 1.6$, and begins to climb with further increase in λ. The experimental data and our correlation both confirm that at 0.2% inlet CO concentration, the exit CO concentration can be reduced to an arbitrarily small value. Our correlation suggests that the minimum in CO concentration is reached at lower λ(1.2) at 2.5% inlet CO concentration than at 1.3% inlet CO concentration.

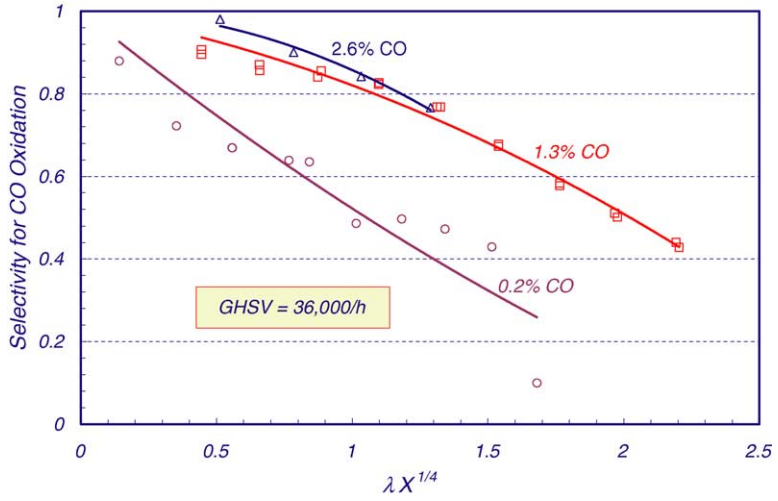

Fig. 6. Selectivity as a function of the reduced parameter.

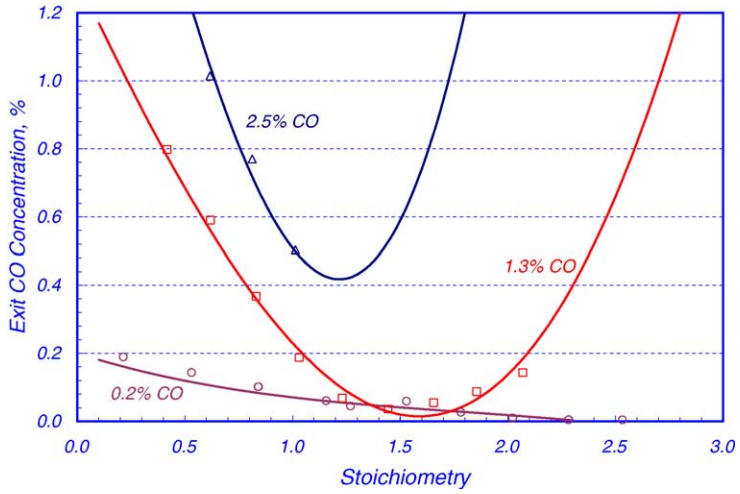

Fig. 7. Comparison of model results (solid lines) to experimental data (cases 1, 2, and 5).

4. Optimum PrOx reactors

As an application of our model, consider a single-stage adiabatic PrOx reactor that uses the Selectra®-PROX I catalyst coated on a 600 cpsi monolith. The inlet temperature of the reformate stream is 100 °C and the space velocity is 30,000–80,000/h so that the selectivity correlation given in Eq. (1) applies. We are interested in determining the operating conditions necessary to reduce the CO concentration to 10 ppm. Fig. 8 shows the calculated oxygen stoichiometry and the corresponding selectivity to meet this target. It indicates that the selectivity for CO oxidation increases with inlet CO concentration, from 0.41 at 0.1% CO to 0.58 at 1% CO. Further increase in inlet CO concentration causes the selectivity to drop slightly. Our calculations indicate that a single-stage adiabatic PrOx reactor cannot meet the 10 ppm target if the inlet CO concentration is greater than 1.05%. For CO concentrations greater than 1.05%, two or more stages are required to meet the 10-ppm target.

Fig. 9 illustrates our concept of a multi-stage PrOx reactor. Air is added at the inlet of each stage to oxidize a portion of CO in the reformate gas at 100 °C inlet temperature. Each stage of the reactor is adiabatic so that the gas temperature rises with addition of air and the consequent exothermic CO and H_2 oxidation reactions. An intercooler downstream of a reactor stage lowers the reformate temperature back to 100 °C. The process of air addition and intercooling is repeated in each stage. We assume that the space velocity in each stage is between 30,000 and 80,000/h so that the added air is completely reacted and the selectivity correlation given in Eq. (1) applies. The objective is to determine the amount of air added in each stage (i.e., oxygen stoichiometry for each

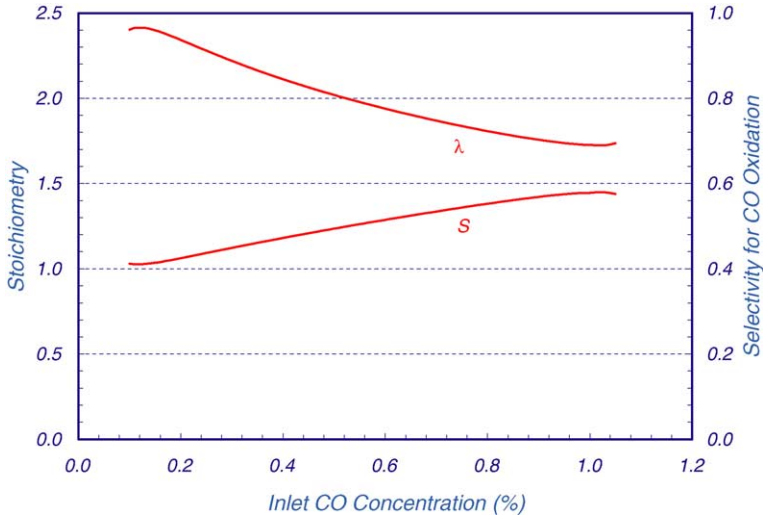

Fig. 8. Selectivity for CO oxidation and stoichiometry in single-stage PrOx reactor.

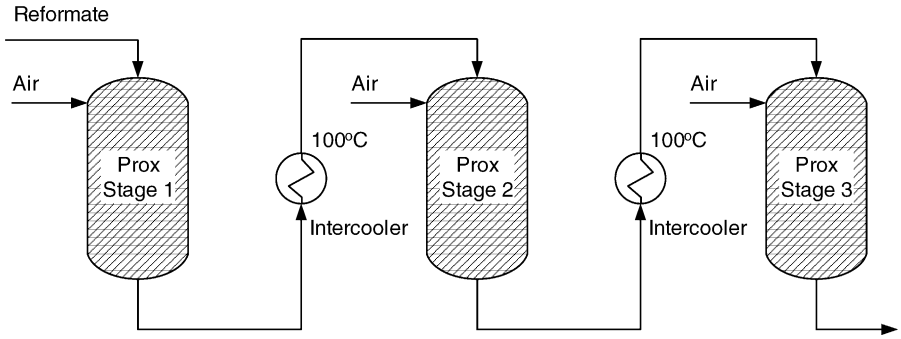

Fig. 9. Multi-stage adiabatic PrOx with intercooling.

stage, λ_i) so that the final CO concentration is 10 ppm. We further seek an optimum combination of λ_i that minimizes the total amount of H_2 consumed in PrOx reactors. Because oxygen is completely reacted, this is equivalent to minimizing the total amount of oxygen in air fed to the reactor stages. Mathematically, this optimization task can be stated as

$$\text{Minimize} \sum_{i=1}^{n} \dot{N}_i^{O_2}$$
$$\text{with } \lambda_i \text{ in } [0, 5]$$
$$\text{such that } X_n \leq 10 \text{ ppm},$$

where X_n is the concentration of CO at the exit of the final reactor stage. From the definition of the oxygen stoichiometry λ_i

$$\dot{N}_i^{O_2} = \left(\frac{\dot{N}_i}{2}\right)\lambda_i X_i \tag{3}$$

where $\dot{N}_i^{O_2}$ is the molar flow rate of oxygen in air added to stage i, $\dot{N}_i$ is the molar flow rate of the reformate stream, and X_i is the concentration of CO in the reformate stream at inlet to stage i. Since oxygen is consumed completely in each reactor stage, it can be shown that CO conversion in stage i (Φ_i) is simply related to the selectivity for CO oxidation (S_i) and oxygen stoichiometry (λ_i) as

$$\Phi_i = \lambda_i S_i \tag{4}$$

Knowing Φ_i, the following equation can be used to calculate CO concentration at exit of stage i (X_{i+1}).

$$X_{i+1} = \frac{X_i}{1 + (79/42)\lambda_i X_i}(1 - \phi_i) \tag{5}$$

We have used a sequential quadratic programming technique for solving the foregoing well-posed nonlinear constrained optimization problem. The results of this optimization for a two-stage reactor are given in Figs. 10–12 for different inlet CO concentrations. At the optimum operating point, Fig. 10 shows that the first stage does more CO conversion than the second stage. The optimal fractional CO conversion in stage one (ϕ_1) is a function of the inlet CO concentration (X_1). Starting at X_1 of 0.5%, Fig. 10 indicates that optimal $\phi_1$initially increases with $X_1$to reach a peak value of 88% at 1.3% inlet CO concentration and then declines slightly as X_1 is raised

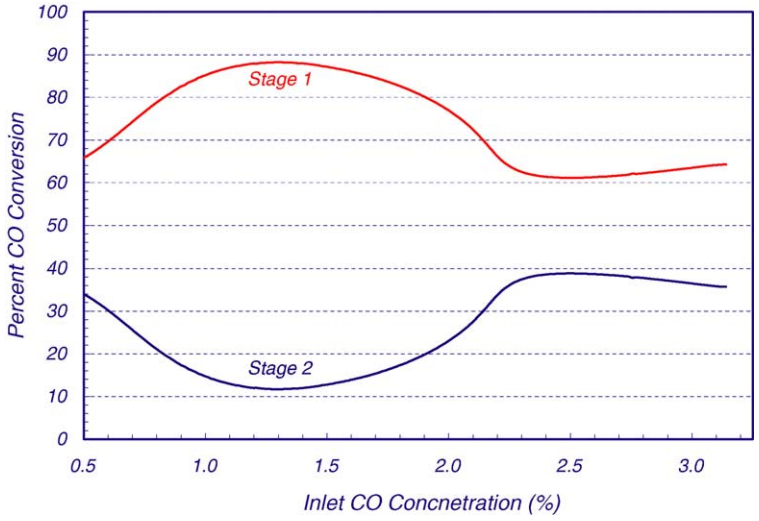

Fig. 10. Optimal conversion in two-stage PrOx reactor.

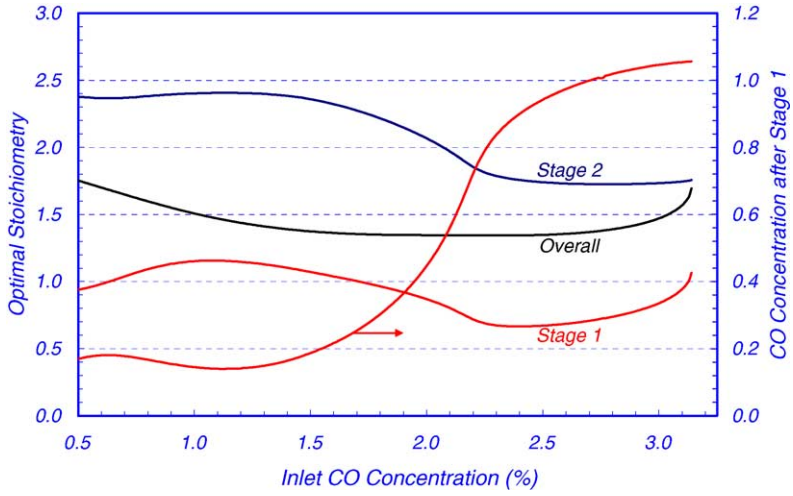

Fig. 11. Optimal stoichiometry for two-stage PrOx reactor.

further. Note that for a two-stage reactor, fractional (ϕ_i) and stage conversions (Φ_i) of CO are related as follows.

$$\phi_1 = \Phi_1$$
$$\phi_2 = (1 - \phi_1)\Phi_2 \quad (6)$$

Fig. 11 shows the CO concentration at the outlet of stage 1 (X_2). It is seen that X_2 increases monotonically with X_1 approaching 1.05% at 3.1% inlet CO concentration. We saw previously that the maximum CO concentration that can be reduced to less than 10 ppm in a single-stage adiabatic reactor is also 1.05%. We therefore conclude that at the maximum CO concentration (3.1%) that can be reduced to less than 10 ppm in a two-stage adiabatic reactor with intercooling, the intermediate CO concentration at the exit from stage 1 is the same as the maximum inlet CO concentration that can be reduced to 10 ppm in a single-stage reactor.

Figs. 11 and 12 show the optimal stoichiometries and selectivities for stages 1 and 2 of the two-stage reactor. It is seen that at optimum operating points, λ_1 is always smaller than λ_2 and S_1 is always greater than S_2. Also included in Figs. 11 and 12 are the overall stoichiometry and selectivity. We define the overall stoichiometry as the ratio of total oxygen in air fed to stages 1 and 2 to the theoretical amount needed to completely oxidize CO in the reformate entering stage 1 of the two-stage reactor. Similarly, the overall selectivity is defined as the fraction of the total amount of oxygen in air fed to stages 1 and 2 that goes into oxidizing CO. The overall λ and S for a two-stage reactor are related to the stage stoichiometries (λ_1 and λ_2) selectivities (S_1 and S_2) and CO conversions (Φ_1 and Φ_2) as

$$\lambda = \lambda_1 + (1 - \Phi_1)\lambda_2$$
$$S = \frac{[1 - (1 - \Phi_1)(1 - \Phi_2)]}{\lambda} \quad (7)$$

Fig. 12 indicates that the overall selectivity generally increases with inlet CO concentration and that a two-stage reactor is capable of reaching a peak selectivity of about 0.75.

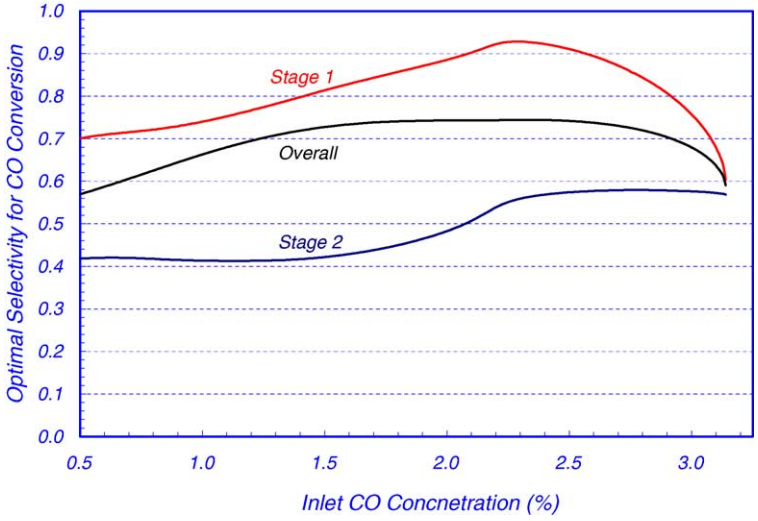

Fig. 12. Optimal selectivity in two-stage PrOx reactor.

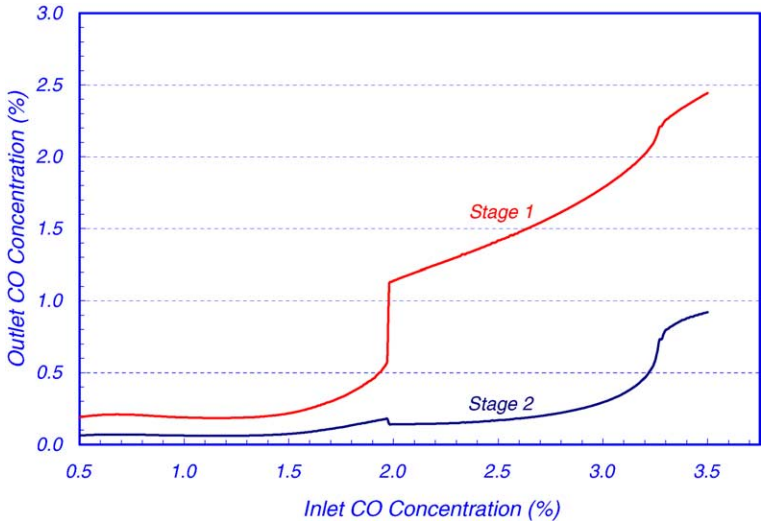

Fig. 13. CO concentration after stages 1 and 2 of three-stage PrOx reactor.

It is worth emphasizing that even though the overall selectivity may increase with inlet CO concentration, it does not imply that hydrogen loss may decrease as CO concentration is increased. In fact the opposite is always true. It can be shown that hydrogen loss (mole%) is related to the overall stoichiometry (λ) and selectivity (S) by the following equation.

$$\frac{\Delta\dot{N}^{H_2}}{\dot{N}} = \lambda(1-S)X_1 \tag{8}$$

Applying this equation to the results presented in Figs. 12 and 13, we see that with a two-stage PrOx, hydrogen loss increases from 0.4 mole% at 0.5% inlet CO concentration to 0.5 mole% at 1% CO, 0.7 mole% at 2% CO, and 1.5 mole% at 3% CO.

We have also used the optimization technique to analyze the performance of a three-stage PrOx reactor and the results are presented in Figs. 13–16. At the optimum operating conditions, Fig. 13 shows the intermediate CO concentrations in the reformate streams after stages 1 and 2 as a function of the CO concentration at the inlet to stage 1 (the CO concentration is always 10 ppm after stage 3).

Fig. 14 presents the optimal fractional CO conversion (ϕ) in the three stages of the reactor. As expected, CO conversion is higher in stages 1 and 2 than in stage 3. For inlet CO concentrations less than 3%, stages 1 and 2 do the bulk of CO conversion while stage 3 does the polishing to meet the 10 ppm target. Note that Eq. (6) also applies to the stages 1 and 2 of the three-stage reactor. In addition, ϕ_3 and Φ_3 are related by the following equation.

$$\phi_3 = (1-\Phi_1)(1-\Phi_2)\Phi_3 \tag{9}$$

Fig. 15 confirms that at all optimum operating conditions, λ_1 and λ_2 are less than λ_3. For optimum process efficiency, it is preferable to operate stages 1 and 2 at sub or near-stoichiometric conditions and introduce excess oxygen in

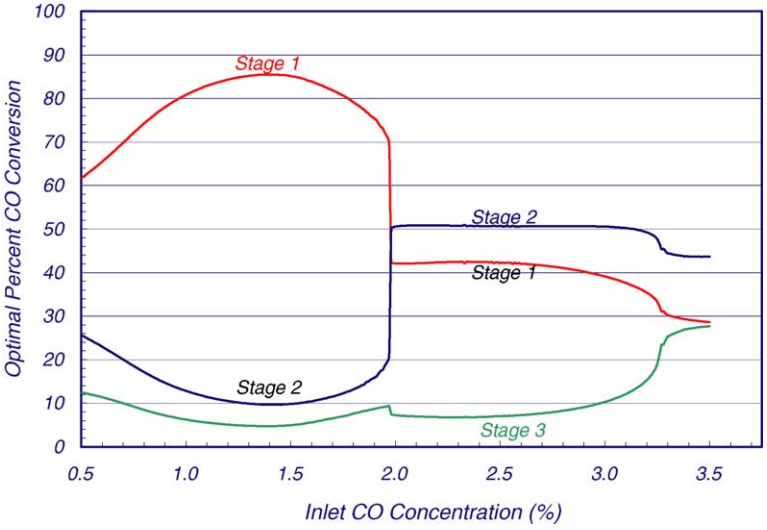

Fig. 14. Optimal CO conversion in three-stage PrOx reactor.

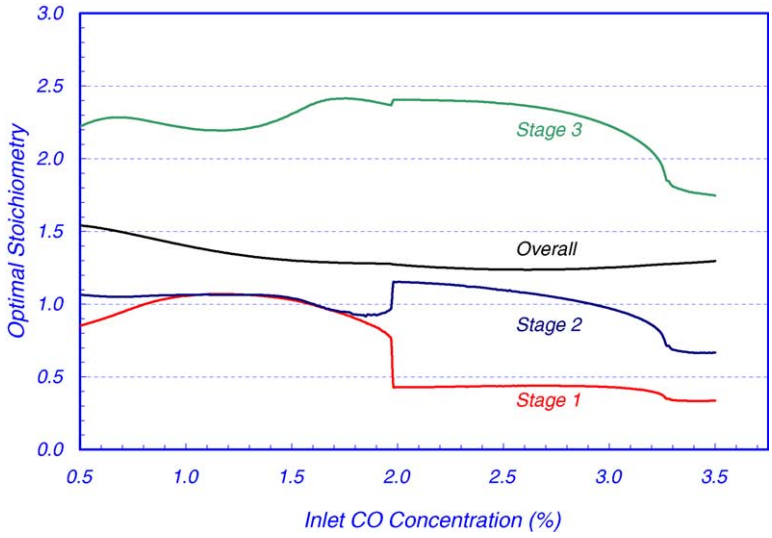

Fig. 15. Optimal stoichiometries for three-stage PrOx reactor.

stage 3 where the CO concentration is the lowest. Also included in Fig. 15 is the overall stoichiometry (λ), which for a three-stage reactor is related to the stage stoichiometries and stage CO conversions as:

$$\lambda = \lambda_1 + (1 - \Phi_1)\lambda_2 + (1 - \Phi_1)(1 - \Phi_2)\lambda_3 \quad (10)$$

Finally, Fig. 16 shows the selectivities for CO oxidation in stages 1, 2 and 3. For inlet CO concentration less than 3%, $S_1 > S_2 > S_3$. The overall selectivity of a three-stage reactor increases with inlet CO concentration, from 0.65 at 0.5% CO to 0.8 at 2.5% CO. There is a slight decrease in the overall selectivity as inlet CO concentration is raised beyond 2.5%. Note that for a three-stage reactor, the overall selectivity (S) is related to the overall stoichiometry (λ) and overall CO conversion (Φ) through the following equation.

$$\lambda S = \Phi = 1 - (1 - \Phi_1)(1 - \Phi_2)(1 - \Phi_3) \quad (11)$$

We have not attempted to determine the maximum inlet CO concentration that can be reduced to 10 ppm in a three-stage reactor because it is likely to be outside the range of validity of our selectivity correlation. However, we suggest that at this upper limit the CO concentration at the outlet of the first stage will be 3.1%, the maximum CO concentration that can be reduced to 10 ppm in a two-stage reactor.

5. Discussion of results

Besides the issues of hardware complexity and controls that are not specifically addressed in this work, the choice of number of PrOx stages is influenced by the maximum CO concentration in the reformate stream at the inlet to PrOx, target CO concentration at PrOx outlet and allowable parasitic loss of hydrogen. We have constructed Figs. 17 and 18 from the results in the last section to directly compare the performance of one, two and three-stage adiabatic PrOx reactors with intercooling between stages. Fig. 17 shows that

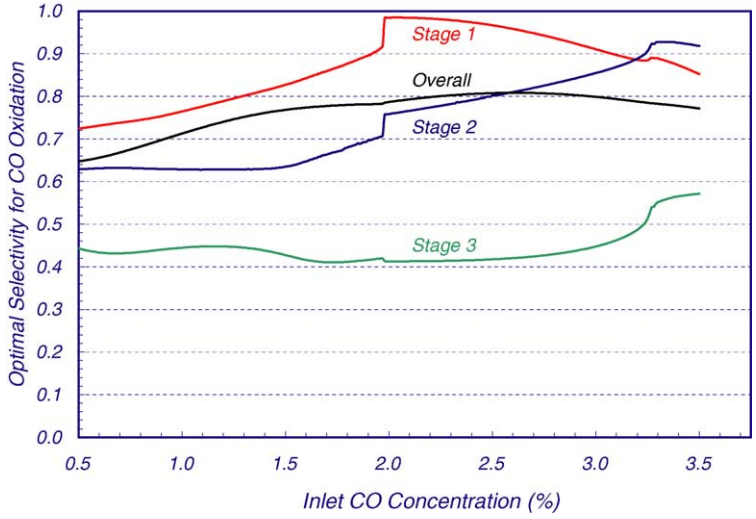

Fig. 16. Optimal selectivity for CO conversion in three-stage PrOx reactor.

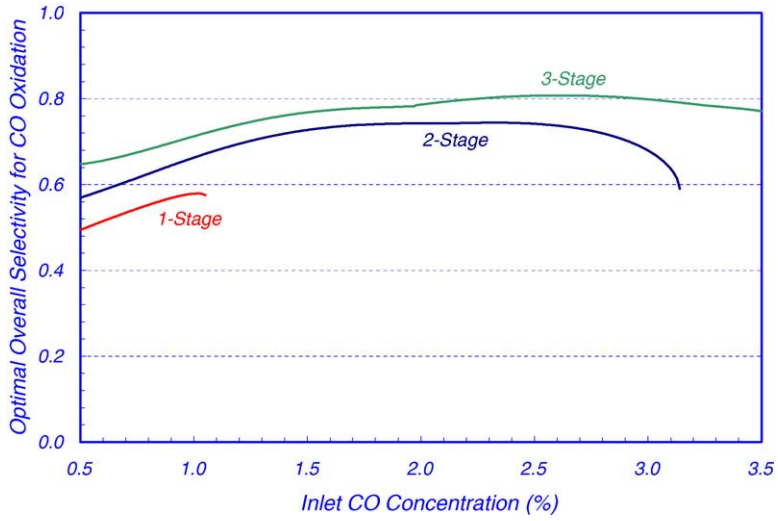

Fig. 17. Comparison of selectivities with one, two and three-stage PrOx reactors.

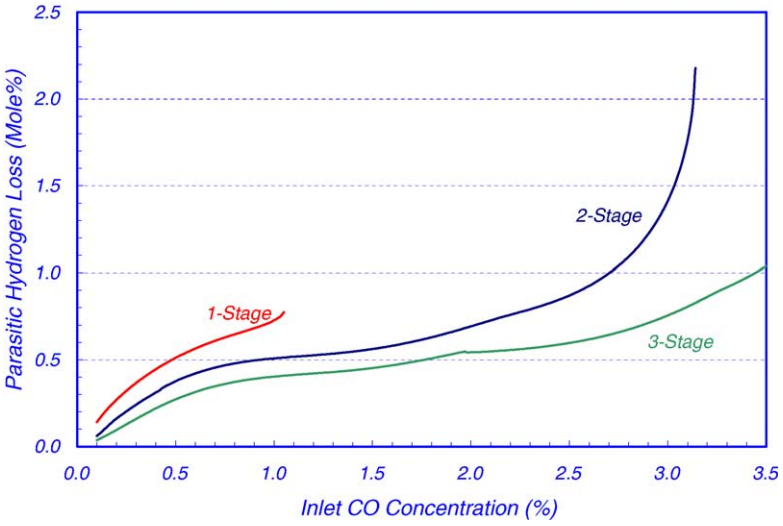

Fig. 18. Minimum parasitic loss of H_2 in one, two and three-stage reactors.

the maximum CO concentration that can be reduced to 10 ppm in a single-stage reactor is limited to 1.05%. Addition of a second stage extends the maximum inlet CO concentration that can be reduced to 10 ppm to 3.1%. Three stages are required if the maximum inlet CO concentration is higher than 3.1%. The maximum selectivity that can be achieved is 0.58 with a one-stage reactor, 0.75 with a two-stage reactor, and 0.81 with a three-stage reactor.

The number of stages affects the parasitic loss of H_2 in the PrOx reactor. In a one-stage reactor, hydrogen loss is almost linearly proportional to the inlet CO concentration (see Fig. 18). At 1% inlet CO concentration, there is a 0.75 mole% loss in H_2 with a one-stage reactor, which can be reduced to 0.5 mole% by adding a second stage. In a two-stage reactor, H_2 loss begins to increase disproportionately with increase in CO concentration beyond 1.75% or so. Insofar as H_2 loss is concerned, the incremental benefit of adding a third stage to a two-stage reactor is marginal for inlet CO concentrations less than 1.75% but can be substantial at higher CO concentrations. For example, at 3% inlet CO concentration the H_2 loss is 2 mole% in a two-stage reactor but only 0.75 mole% in a three-stage reactor.

6. Summary and conclusions

It is feasible to conduct preferential oxidation of CO on a noble-metal catalyst coated ceramic monolith at 100 °C to produce a PEMFC quality gas at space velocities in excess of 30,000/h. Our experimental data taken under these conditions indicates that oxygen is completely consumed in tests with 0.2–2.5% inlet CO concentrations and 0.4–2.5 oxygen

stoichiometry. The measured selectivity for CO oxidation is weakly dependent on the moisture content, suggesting that the reverse water gas shift reaction does not significantly affect CO conversion on the Selectra®-PROX I catalyst at temperatures between 100 and 300 °C. The measured selectivity for CO oxidation (S) is found to be a strong function of inlet CO concentration (X) and oxygen stoichiometry (λ). For given inlet CO concentration, the selectivity always decreases with increase in oxygen stoichiometry.

We developed an empirical correlation for selectivity for CO oxidation as a function of the inlet CO concentration and a reduced parameter $\lambda X^{1/4}$. We used this correlation in a model to determine the optimum operating conditions of a PrOx reactor that reduces the CO concentration to a specified level (presumably determined by the CO tolerance of the PEMFC anode catalyst) while minimizing parasitic H_2 loss (which amounts to maximizing the process efficiency). The model was used to determine the maximum inlet CO concentration that can be reduced to 10 ppm in one, two and three-stage adiabatic reactors with intercooling. These were found to be 1.05% for a single-stage reactor, 3.1% for a two-stage reactor, and higher than the probable limit of validity of our correlation for a three-stage reactor. Regardless of the number of stages, results from our model show that the overall selectivity of the PrOx reactor generally increases with inlet CO concentration. Adding a second stage to a single-stage reactor reduces the parasitic H_2 loss to 0.5 mole% from 0.75 mole% at 1% inlet CO. In terms of reducing H_2 loss, there is a clear benefit of adding a third stage to a two-stage reactor if the inlet CO concentration is higher than 1.75%.

Acknowledgements

This work was supported by the U.S. Department of Energy's Office of Energy Efficiency and Renewables, Office of Hydrogen, Fuel Cells and Infrastructure Technologies and by the Graduate College at the Illinois Institute of Technology. Dr. Nancy Garland is the program manager at U.S.D.O.E.

References

[1] R.K. Ahluwalia, X. Wang, A. Rousseau, R. Kumar, J. Power Sources 130 (2004) 192.
[2] Hydrogen Posture Plan: An Integrated Research, Development, and Demonstration Plan, February 2004.
[3] E.D. Doss, R. Kumar, R.K. Ahluwalia, M. Krumpelt, J. Power Sources 102 (2002) 1.
[4] T.E. Springer, T. Rockward, T.A. Zawodzinski, S. Gottesfeld, J. Electrochem. Soc. 148 (2001) 11.
[5] R.K. Ahluwalia, E.D. Doss, R. Kumar, J. Power Sources 117 (2003) 45.
[6] J. Wagner, H. Takeda, 2003 Fuel Cell Seminar, 3–7 November, 2003, p. 925.
[7] A. LaVen, Hydrogen, Fuel Cells and Infrastructure Technologies, DOE FY2003 Progress Report, 2003.
[8] Thin Supported Pd-Alloy Membranes for Hydrogen Purification, ETSU Report F/02/00034/REP, 1995.
[9] M.J. Kahlich, H.A. Gasteiger, J. New Mater. Electrochem. Syst. 1 (1998) 39–46.
[10] S.H. Oh, R.M. Sinkevitch, J. Catal. 142 (1993) 253–262.
[11] C.D. Dudfield, R. Chen, P.L. Adcock, J. Power Sources 85 (2000) 237–244.
[12] C.D. Dudfield, R. Chen, P.L. Adcock, J. Power Sources 86 (2000) 214–222.